ÉCOLE POLYTECHNIQUE
FÉDÉRALE DE LAUSANNE

# Sparse stochastic processes

## Part 2:
## Recovery of sparse signals

Prof. Michael Unser, LIB

EPFL Doctoral School EDEE, Course EE-726, Spring 2017

## Table of content

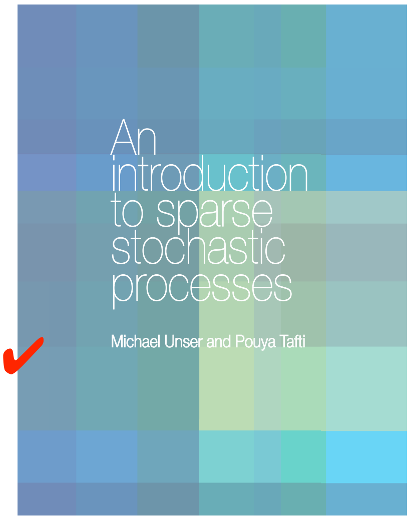


1. Introduction ✔
2. Roadmap to the monograph ✔
3. Mathematical context and background
4. Continuous-domain innovation models ✔
5. Operators and their inverses
6. Splines and wavelets
7. Sparse stochastic processes ✔
8. Sparse representations
9. Infinite divisibility and transform-domain statistic
10. **Recovery of sparse signals**
11. Wavelet-domain methods

# CONTENT

- **10.1 Discretization of inverse problem**
- **10.2 MAP estimation and regularization**
- **10.3 MAP reconstruction of biomedical images**
  - Deconvolution of fluorescent micrographs
  - Magnetic resonance imaging
  - X-ray tomography



# Resolution of linear inverse problems

- Linear forward model

$$\mathbf{y} = \mathbf{H}\mathbf{s} + \mathbf{n}$$

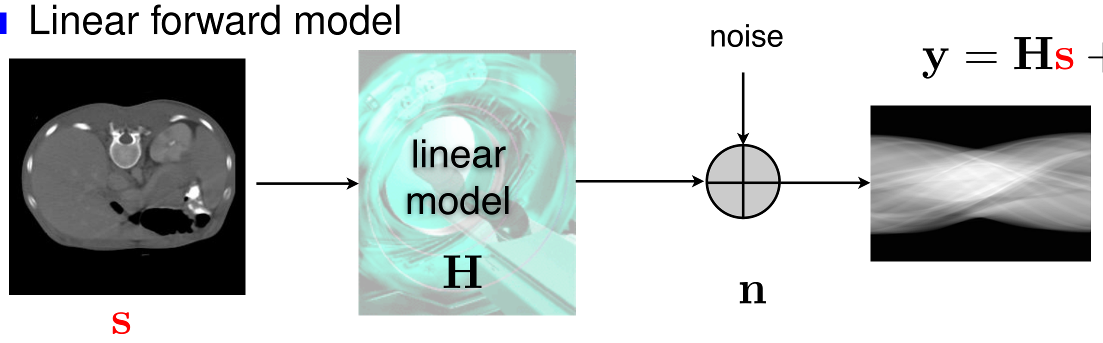


Ill-posed inverse problem: recover $\mathbf{s}$ from noisy measurements $\mathbf{y}$

- Reconstruction as an optimization problem

**Bayesian prior** $-\log p_S(\mathbf{s})$

$$\mathbf{s}^\star = \mathrm{argmin} \underbrace{\|\mathbf{y} - \mathbf{H}\mathbf{s}\|_2^2}_{\text{data consistency}} + \underbrace{\lambda\mathcal{R}(\mathbf{s})}_{\text{regularization}}$$

**Gaussian-noise likelihood** $-\log p_{Y|S}(\mathbf{n})$

# Brief review of compressed sensing (CS)

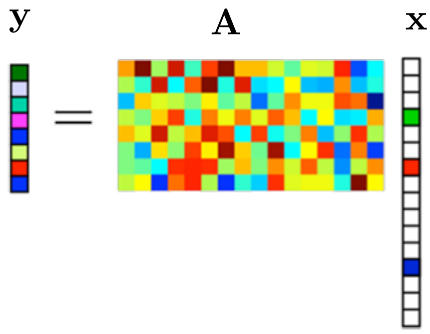




# Theory of compressive sensing

- Generalized sampling setting (after discretization)
  - Linear inverse problem: $\mathbf{y} = \mathbf{H}\mathbf{s} + \mathbf{n}$
  - Sparse representation of signal: $\mathbf{s} = \mathbf{W}\mathbf{x}$ with $\|\mathbf{x}\|_0 = K \ll N_x$
  - Equivalent $N_y \times N_x$ **sensing matrix** : $\mathbf{A} = \mathbf{H}\mathbf{W}$
- Formulation of ill-posed recovery problem when $2K < N_y \ll N_x$

(P0) $\min_{\mathbf{x}} \|\mathbf{y} - \mathbf{A}\mathbf{x}\|_2^2$ subject to $\|\mathbf{x}\|_0 \leq K$

- Theoretical result

Under suitable conditions on $\mathbf{A}$ (e.g., restricted isometry), the solution is unique and the recovery problem (P0) is equivalent to:

(P1) $\min_{\mathbf{x}} \|\mathbf{y} - \mathbf{A}\mathbf{x}\|_2^2$ subject to $\|\mathbf{x}\|_1 \leq C_1$

(P1') $\min_{\mathbf{x}} \|\mathbf{x}\|_1$ subject to $\|\mathbf{y} - \mathbf{A}\mathbf{x}\|_2^2 \leq \sigma^2$

[Donoho et al., 2005
Candès-Tao, 2006, ...]

# Constrained $l_1$ minimization $\Rightarrow$ sparsifying effect

- Discrete signal to reconstruct: $x = (x[n])_{n \in \mathbb{Z}}$
- Sensing operator $\mathrm{H} : \ell_1(\mathbb{Z}) \to \mathbb{R}^M$
  $x \mapsto \mathbf{z} = \mathrm{H}\{x\} = (\langle x, h_1 \rangle, \dots, \langle x, h_M \rangle)$ with $h_m \in \ell_\infty(\mathbb{Z})$
- Closed convex set in measurement space: $\mathcal{C} \subset \mathbb{R}^M$

**Representer theorem for constrained $\ell_1$ minimization**

(P1) $$\mathcal{V} = \arg \min_{x \in \ell_1(\mathbb{Z})} \|x\|_{\ell_1} \quad \text{s.t.} \quad \mathrm{H}\{x\} \in \mathcal{C}$$

is convex, weak*-compact with extreme points of the form

$$x_{\text{sparse}}[\cdot] = \sum_{k=1}^{K} a_k \delta[\cdot - n_k] \quad \text{with} \quad K = \|x_{\text{sparse}}\|_0 \leq M.$$

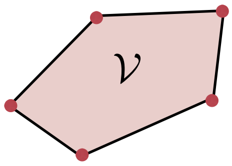


If CS condition is satisfied,
then solution is unique

(U.-Fageot-Gupta *IEEE Trans. Info. Theory*, Sept. 2016)



# Controlling sparsity

Measurement model: $y_m = \langle h_m, x \rangle + n[m], \quad m = 1, \dots, M$

$$x_{\text{sparse}} = \arg \min_{x \in \ell_1(\mathbb{Z})} \left( \sum_{m=1}^{M} \left| y_m - \langle h_m, x \rangle \right|^2 + \lambda \|x\|_{\ell_1} \right)$$

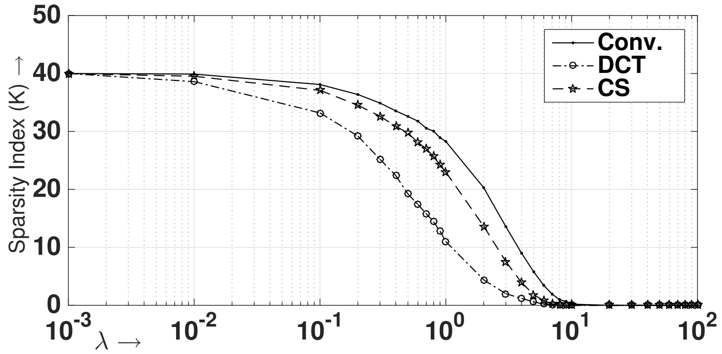

# Geometry of $l_2$ vs. $l_1$ minimization

- Prototypical inverse problem

$$\min_{\mathbf{x}} \left\{ \|\mathbf{y}-\mathbf{H}\mathbf{x}\|_{\ell_2}^2 + \lambda \|\mathbf{x}\|_{\ell_2}^2 \right\} \Leftrightarrow \min_{\mathbf{x}} \|\mathbf{x}\|_{\ell_2} \text{ subject to } \|\mathbf{y}-\mathbf{H}\mathbf{x}\|_{\ell_2}^2 \le \sigma^2$$

$$\min_{\mathbf{x}} \left\{ \|\mathbf{y}-\mathbf{H}\mathbf{x}\|_{\ell_2}^2 + \lambda \|\mathbf{x}\|_{\ell_1} \right\} \Leftrightarrow \min_{\mathbf{x}} \|\mathbf{x}\|_{\ell_1} \text{ subject to } \|\mathbf{y}-\mathbf{H}\mathbf{x}\|_{\ell_2}^2 \le \sigma^2$$

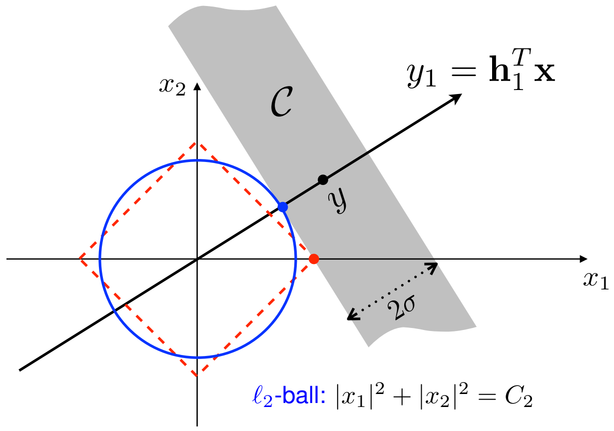




# Geometry of $l_2$ vs. $l_1$ minimization

- Prototypical inverse problem

$$\min_{\mathbf{x}} \left\{ \|\mathbf{y}-\mathbf{H}\mathbf{x}\|_{\ell_2}^2 + \lambda \|\mathbf{x}\|_{\ell_2}^2 \right\} \Leftrightarrow \min_{\mathbf{x}} \|\mathbf{x}\|_{\ell_2} \text{ subject to } \|\mathbf{y}-\mathbf{H}\mathbf{x}\|_{\ell_2}^2 \le \sigma^2$$

$$\min_{\mathbf{x}} \left\{ \|\mathbf{y}-\mathbf{H}\mathbf{x}\|_{\ell_2}^2 + \lambda \|\mathbf{x}\|_{\ell_1} \right\} \Leftrightarrow \min_{\mathbf{x}} \|\mathbf{x}\|_{\ell_1} \text{ subject to } \|\mathbf{y}-\mathbf{H}\mathbf{x}\|_{\ell_2}^2 \le \sigma^2$$

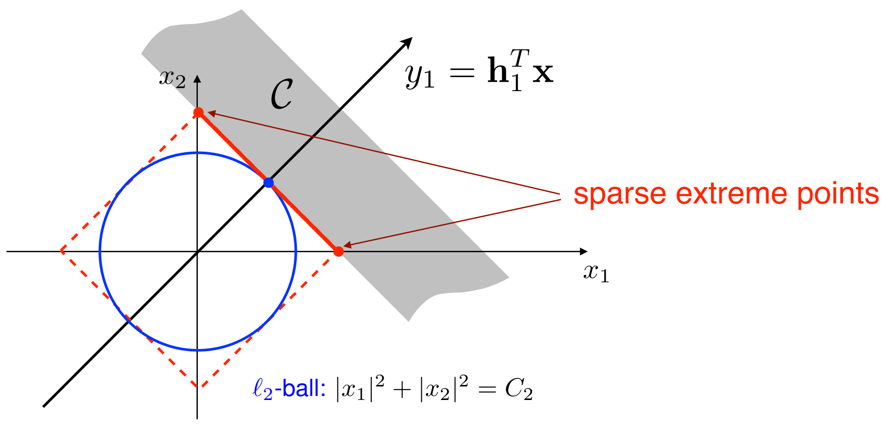


Configuration for **non-unique** $\ell_1$ solution

## Sparsity and non-quadratic regularization

$$\mathbf{s}^\star = \text{argmin} \underbrace{\|\mathbf{g} - \mathbf{H}\mathbf{s}\|_2^2}_{\text{data consistency}} + \underbrace{\lambda \mathcal{R}(\mathbf{s})}_{\text{regularization}}$$

- $\ell_1$ regularization (Total variation)

**State-of-the-art in MRI**

[Rudin-Osher, 1992; Lustig et al., 2007, ...]

$$\mathcal{R}(\mathbf{s}) = \|\mathbf{L}\mathbf{s}\|_{\ell_1} \text{ with } \mathbf{L}\text{: gradient}$$

Iterative reweighted least squares (IRLS) or FISTA

- General potential functions

$$\mathcal{R}(\mathbf{s}) = \sum_n \Phi\big([\mathbf{L}\mathbf{s}]_n\big)$$

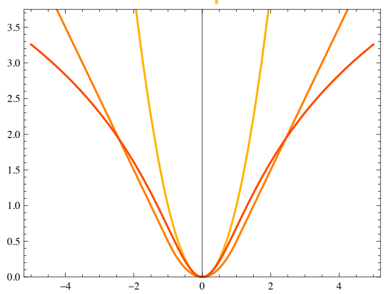




## 10.1 DISCRETIZATION OF INVERSE PROBLEMS

- Two aspects
  - Discretization of **physical** forward model
  - Discretization of **probability** model

How?

By projection on a suitable set of basis functions

$$\{\beta_{\boldsymbol{k}}(\boldsymbol{r})\}_{\boldsymbol{k}\in\Omega}$$

# Generalized innovation model

Theoretical framework: Gelfand's theory of generalized stochastic processes

2 Specification of inverse operator

**Functional analysis solution of SDE**

3

**Very easy ! (after solving 1. & 2.)**

***innovation process***

***sparse stochastic process***

$X = \langle \varphi, w \rangle$

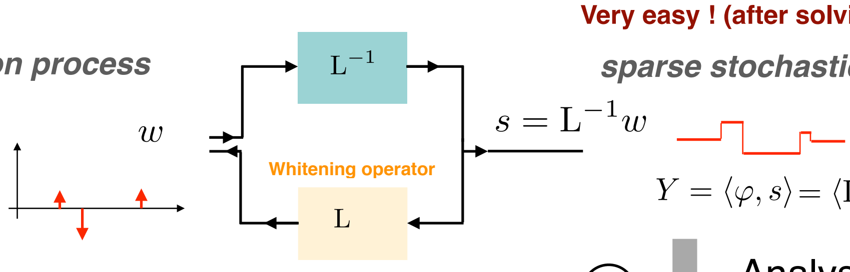


$Y = \langle \varphi, s \rangle = \langle \mathrm{L}^{-1*} \varphi, w \rangle$

4 Analysis step

Lévy exponent: $f(\omega)$

1 Characterization of continuous-domain white noise

**Higher mathematics: generalized functions (Schwartz)**

**measures on topological vector spaces**

Minlos-Bochner and Lévy-Khintchine theorems

Regularization operator vs. wavelet analysis

**Easy when:** $\psi_i = \mathrm{L}^* \phi_i$



# Discretization of reconstruction problem

Spline-like reconstruction model: $s(\boldsymbol{r}) = \sum_{\boldsymbol{k} \in \Omega} s[\boldsymbol{k}] \beta_{\boldsymbol{k}}(\boldsymbol{r}) \quad \longleftrightarrow \quad \mathbf{s} = (s[\boldsymbol{k}])_{\boldsymbol{k} \in \Omega}$

- Innovation model

$$\begin{aligned} \mathrm{L}s &= w \\ s &= \mathrm{L}^{-1} w \end{aligned}$$

Discretization

$\mathbf{u} = \mathbf{L}\mathbf{s}$ (matrix notation)

$p_U$ is part of **infinitely divisible** family

- Physical model: image formation and acquisition

$$y_m = \int_{\mathbb{R}^d} s_1(\boldsymbol{x}) \eta_m(\boldsymbol{x}) \mathrm{d}\boldsymbol{x} + n[m] = \langle s_1, \eta_m \rangle + n[m], \quad (m = 1, \ldots, M)$$

$$\mathbf{y} = \mathbf{y}_0 + \mathbf{n} = \mathbf{H}\mathbf{s} + \mathbf{n}$$

$\mathbf{n}$: i.i.d. noise with pdf $p_N$

$$[\mathbf{H}]_{m,\boldsymbol{k}} = \langle \eta_m, \beta_{\boldsymbol{k}} \rangle = \int_{\mathbb{R}^d} \eta_m(\boldsymbol{r}) \beta_{\boldsymbol{k}}(\boldsymbol{r}) \mathrm{d}\boldsymbol{r}: \quad (M \times K) \text{ system matrix}$$

## Posterior probability distribution

$$p_{S|Y}(\mathbf{s}|\mathbf{y}) = \frac{p_{Y|S}(\mathbf{y}|\mathbf{s})p_S(\mathbf{s})}{p_Y(\mathbf{y})} = \frac{p_N(\mathbf{y}-\mathbf{Hs})p_S(\mathbf{s})}{p_Y(\mathbf{y})} \qquad \text{(Bayes' rule)}$$

$$= \frac{1}{Z} p_N(\mathbf{y}-\mathbf{Hs})p_S(\mathbf{s})$$

$$\mathbf{u} = \mathbf{Ls} \qquad \Rightarrow \qquad p_S(\mathbf{s}) \propto p_U(\mathbf{Ls}) \approx \prod_{\boldsymbol{k}\in\Omega} p_U\left([\mathbf{Ls}]_{\boldsymbol{k}}\right)$$

- Additive white Gaussian noise scenario (AWGN)

$$p_{S|Y}(\mathbf{s}|\mathbf{y}) \propto \exp\left(-\frac{\|\mathbf{y}-\mathbf{Hs}\|^2}{2\sigma^2}\right) \prod_{\boldsymbol{k}\in\Omega} p_U\left([\mathbf{Ls}]_{\boldsymbol{k}}\right)$$

... and then take the log and maximize ...



## General form of MAP estimator

$$\mathbf{s}_{\mathrm{MAP}} = \operatorname{argmin}\left(\tfrac{1}{2}\|\mathbf{y}-\mathbf{Hs}\|_2^2 + \sigma^2 \textstyle\sum_n \Phi_U([\mathbf{Ls}]_n)\right)$$

- Gaussian: $p_U(x) = \frac{1}{\sqrt{2\pi}\sigma_0} e^{-x^2/(2\sigma_0^2)}$ $\Rightarrow$ $\Phi_U(x) = \frac{1}{2\sigma_0^2}x^2 + C_1$
- Laplace: $p_U(x) = \frac{\lambda}{2} e^{-\lambda|x|}$ $\Rightarrow$ $\Phi_U(x) = \lambda|x| + C_2$
- Student: $p_U(x) = \frac{1}{B\left(r, \frac{1}{2}\right)} \left(\frac{1}{x^2+1}\right)^{r+\frac{1}{2}}$ $\Rightarrow$ $\Phi_U(x) = \left(r+\frac{1}{2}\right)\log(1+x^2) + C_3$

Sparser

Potential: $\Phi_U(x) = -\log p_U(x)$

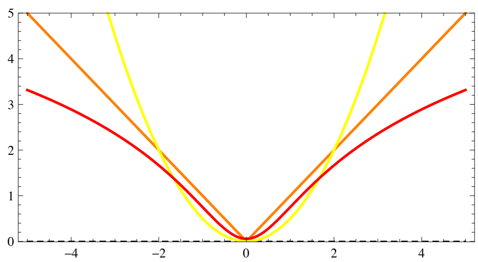

| $p_X(x)$ | $\Phi_X(x) = -\log p_X(x)$ as $x \to 0$ | $\Phi_X(x)$ as $x \to \pm\infty$ | Smooth | Convex |
|---|---|---|---|---|
| Gaussian | $a_0 + \frac{x^2}{2\sigma^2}$ | $a_0 + \frac{x^2}{2\sigma^2}$ | Yes | Yes |
| Laplace ($\lambda \in \mathbb{R}^+$) | $a_0 + \lambda\|x\|$ | $a_0 + \lambda\|x\|$ | No | Yes |
| Sym Gamma $r \in \mathbb{R}^+$ | $\begin{cases} \log(a_0' + a_r'\|x\|^{2r-1} + O(x^2)), & r < 3/2 \\ a_0 + \frac{x^2}{4r-6} + O(\|x\|^{\min(4,2r-1)}), & r > 3/2 \end{cases}$ | $b_0 + \|x\| - (r-1)\log\|x\|$ | No | No |
| Hyperbolic secant | $a_0 + \frac{\pi^2 x^2}{8\sigma_0^2} + O(x^4)$ | $-\log\sigma_0 + \frac{\pi}{2\sigma_0}\|x\|$ | Yes | Yes |
| Meixner $r, s \in \mathbb{R}^+$ | $a_0 + \frac{\psi^{(1)}(r/2)}{4s^2}x^2 + O(x^4)$ | $b_0 + \frac{\pi}{2s}\|x\| - (r-1)\log\|x\|$ | Yes | No |
| Cauchy $s \in \mathbb{R}^+$ | $a_0 + \frac{x^2}{s^2} + O(x^4)$ | $b_0 - \log s + 2\log\|x\|$ | Yes | No |
| Sym Student $r \in \mathbb{R}^+$ | $a_0 + \left(r + \frac{1}{2}\right)x^2 + O(x^4)$ | $b_0 + (2r+1)\log\|x\|$ | Yes | No |
| S$\alpha$S, $\alpha \in (0,2], s \in \mathbb{R}^+$ | $a_0 + \frac{\Gamma(\frac{3}{\alpha})}{2s^2\Gamma(\frac{1}{\alpha})}x^2 + O(x^4)$ | $b_0 - \alpha\log s + (\alpha+1)\log\|x\|$ | Yes | No |

$\Gamma(z)$ and $\psi^{(1)}(r)$ are Euler's gamma and first-order poly-gamma functions, respectively (see Appendix C).

**Table 10.1** Asymptotic behavior of the potential function $\Phi_X(x)$ for the infinite-divisible distributions in Table 4.1.



# LMMSE / Gaussian solution

$$\mathbf{s}_{\text{MAP}} = \arg\min_{\mathbf{s}\in\mathbb{R}^K} \mathcal{C}_2(\mathbf{s},\mathbf{y}) \quad \text{with} \quad \mathcal{C}_2(\mathbf{s},\mathbf{y}) = \frac{1}{2}\|\mathbf{y}-\mathbf{H}\mathbf{s}\|_2^2 + \sigma^2\frac{1}{2}\|\mathbf{L}_{\text{G}}\mathbf{s}\|_2^2$$

$$\mathbf{L}_{\text{G}} = \mathbf{C}_{ss}^{-1/2} \text{ where } \mathbf{C}_{ss} = \mathbb{E}\{\mathbf{s}\mathbf{s}^T\}$$

$$\frac{\partial\mathcal{C}_2(\mathbf{s},\mathbf{y})}{\partial\mathbf{s}} = -\mathbf{H}^T(\mathbf{y}-\mathbf{H}\mathbf{s}) + \sigma^2\mathbf{L}_{\text{G}}^T\mathbf{L}_{\text{G}}\mathbf{s} = \mathbf{0}$$

$$\Rightarrow \qquad \mathbf{s}_{\text{MAP}}(\mathbf{y}) = \left(\mathbf{H}^T\mathbf{H} + \sigma^2\mathbf{L}_{\text{G}}^T\mathbf{L}_{\text{G}}\right)^{-1}\mathbf{H}^T\mathbf{y}$$

- Equivalence with LMMSE solution (Wiener filter)

$$\mathbf{s}_{\text{LMMSE}}(\mathbf{y}) = \mathbf{C}_{ss}\mathbf{H}^T\left(\mathbf{H}\mathbf{C}_{ss}\mathbf{H}^T + \mathbf{C}_{nn}\right)^{-1}\mathbf{y}$$

$$\mathbf{C}_{ss}^{-1} = \mathbf{L}_{\text{G}}^T\mathbf{L}_{\text{G}} \quad \text{and} \quad \mathbf{C}_{nn} = \mathbb{E}\{\mathbf{n}\mathbf{n}^T\} = \sigma^2\mathbf{I}$$

$$\mathbf{H}^T\mathbf{H}\mathbf{C}_{ss}\mathbf{H}^T + \sigma^2\mathbf{C}_{ss}^{-1}\mathbf{C}_{ss}\mathbf{H}^T = \mathbf{H}^T\mathbf{H}\mathbf{C}_{ss}\mathbf{H}^T + \sigma^2\mathbf{H}^T$$

$$\left(\mathbf{H}^T\mathbf{H} + \sigma^2\mathbf{C}_{ss}^{-1}\right)\mathbf{C}_{ss}\mathbf{H}^T = \mathbf{H}^T\left(\mathbf{H}\mathbf{C}_{ss}\mathbf{H}^T + \sigma^2\mathbf{I}\right)$$

$$\mathbf{C}_{ss}\mathbf{H}^T\left(\mathbf{H}\mathbf{C}_{ss}\mathbf{H}^T + \sigma^2\mathbf{I}\right)^{-1} = \left(\mathbf{H}^T\mathbf{H} + \sigma^2\mathbf{C}_{ss}^{-1}\right)^{-1}\mathbf{H}^T$$

# Proximal operator: pointwise denoiser

$$\mathrm{prox}_{\Phi_U}(y;\sigma^2) = \arg\min_{u\in\mathbb{R}} \frac{1}{2}|y-u|^2 + \sigma^2\Phi_U(u)$$

$\tilde{u} = \mathrm{prox}_{\Phi_U}(y;1)$

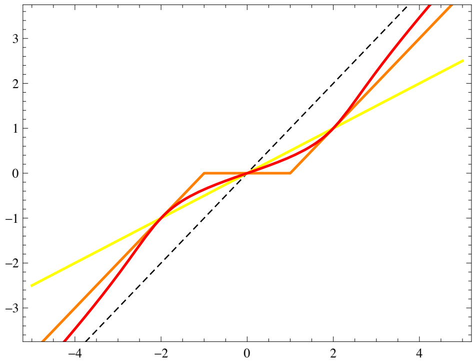


$\sigma^2\Phi_U(u)$

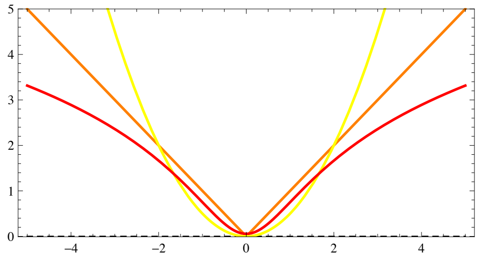


- linear attenuation — $\ell_2$ minimization
- soft-threshold — $\ell_1$ minimization
- shrinkage function $\approx$ $\ell_p$ relaxation for $p \to 0$



# Maximum a posteriori (MAP) estimation

- Constrained optimization formulation

Auxiliary **innovation** variable: $\mathbf{u} = \mathbf{L}\mathbf{s}$

$$\mathbf{s}_{\mathrm{MAP}} = \arg\min_{\mathbf{s}\in\mathbb{R}^K} \left( \frac{1}{2}\|\mathbf{y}-\mathbf{H}\mathbf{s}\|_2^2 + \sigma^2 \sum_n \Phi_U([\mathbf{u}]_n) \right) \text{ subject to } \mathbf{u} = \mathbf{L}\mathbf{s}$$

- Augmented Lagrangian method

Quadratic penalty term: $\frac{\mu}{2}\|\mathbf{L}\mathbf{s}-\mathbf{u}\|_2^2$

Lagrange multiplier vector: $\boldsymbol{\alpha}$

$$\mathcal{L}_{\mathcal{A}}(\mathbf{s},\mathbf{u},\boldsymbol{\alpha}) = \frac{1}{2}\|\mathbf{g}-\mathbf{H}\mathbf{s}\|_2^2 + \sigma^2\sum_n \Phi_U([\mathbf{u}]_n) + \boldsymbol{\alpha}^T(\mathbf{L}\mathbf{s}-\mathbf{u}) + \frac{\mu}{2}\|\mathbf{L}\mathbf{s}-\mathbf{u}\|_2^2$$

# Alternating direction method of multipliers (ADMM)

$$\mathcal{L}_{\mathcal{A}}(\mathbf{s},\mathbf{u},\boldsymbol{\alpha}) = \frac{1}{2}\|\mathbf{g}-\mathbf{H}\mathbf{s}\|_2^2 + \sigma^2 \sum_n \Phi_U([\mathbf{u}]_n) + \boldsymbol{\alpha}^T(\mathbf{L}\mathbf{s}-\mathbf{u}) + \frac{\mu}{2}\|\mathbf{L}\mathbf{s}-\mathbf{u}\|_2^2$$

Sequential minimization

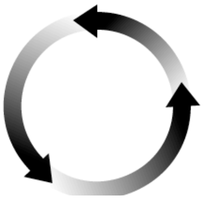

$$\mathbf{s}^{k+1} \leftarrow \arg\min_{\mathbf{s}\in\mathbb{R}^N} \mathcal{L}_{\mathcal{A}}(\mathbf{s},\mathbf{u}^k,\boldsymbol{\alpha}^k)$$

$$\boldsymbol{\alpha}^{k+1} = \boldsymbol{\alpha}^k + \mu\left(\mathbf{L}\mathbf{s}^{k+1}-\mathbf{u}^k\right)$$

$$\mathbf{u}^{k+1} \leftarrow \arg\min_{\mathbf{u}\in\mathbb{R}^N} \mathcal{L}_{\mathcal{A}}(\mathbf{s}^{k+1},\mathbf{u},\boldsymbol{\alpha}^{k+1})$$

**Linear inverse problem:** $\mathbf{s}^{k+1} = \left(\mathbf{H}^T\mathbf{H}+\mu\mathbf{L}^T\mathbf{L}\right)^{-1}\left(\mathbf{H}^T\mathbf{y}+\mathbf{z}^{k+1}\right)$

with $\mathbf{z}^{k+1} = \mathbf{L}^T\left(\mu\mathbf{u}^k-\boldsymbol{\alpha}^k\right)$

**Nonlinear denoising:** $\mathbf{u}^{k+1} = \mathrm{prox}_{\Phi_U}\left(\mathbf{L}\mathbf{s}^{k+1}+\frac{1}{\mu}\boldsymbol{\alpha}^{k+1};\frac{\sigma^2}{\mu}\right)$

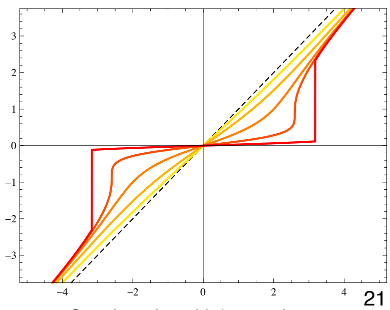


Cauchy prior with increasing $s_0$

- Proximal operator taylored to stochastic model

$$\mathrm{prox}_{\Phi_U}(y;\lambda) = \arg\min_u \frac{1}{2}|y-u|^2 + \lambda\Phi_U(u)$$



# 10.3 RECONSTRUCTION OF BIOMEDICAL IMAGES

- Common image model and numerical set-up
  - $\frac{1}{|\boldsymbol{\omega}|^\gamma}$ spectral decay $\longleftrightarrow$ $(-\Delta)^{\frac{\gamma}{2}} s = w$ (self-similar image model)
  - Robust localization/decoupling $\mathbf{L}$: discrete gradient magnitude (rotation invariant)
  - Three flavors of potentials:

    $|x|^2$ (Gaussian), $|x|$ (Laplacian), $\log(x^2+\epsilon)$ (Student)
- Deconvolution of fluorescent micrographs
- Magnetic resonance imaging
- X-ray tomography

# Relevance of self-similariy for bio-imaging

- Fractals and physiology


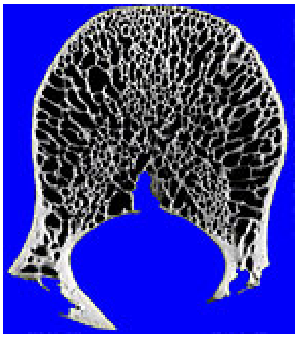

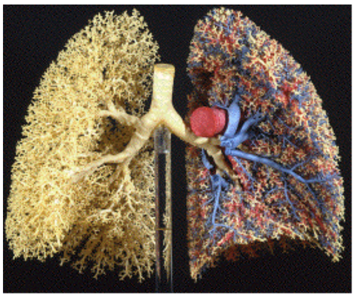
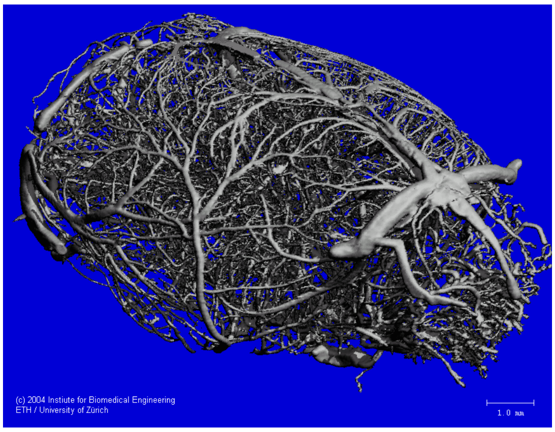




# Deconvolution of fluorescence micrographs

- Physical model of a diffraction-limited microscope

$$g(x,y,z) = (h_{3\mathrm{D}} * s)(x,y,z)$$

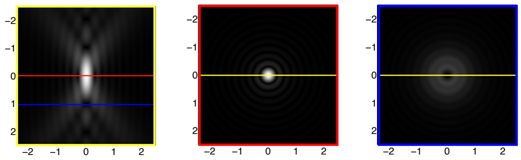

3-D point spread function (PSF)

$$h_{3\mathrm{D}}(x,y,z) = I_0 \left| p_\lambda \left( \tfrac{x}{M}, \tfrac{y}{M}, \tfrac{z}{M^2} \right) \right|^2$$

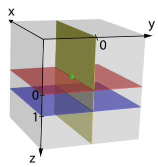


$$p_\lambda(x,y,z) = \int_{\mathbb{R}^2} P(\omega_1,\omega_2) \exp\left( \mathrm{j}2\pi z \frac{\omega_1^2+\omega_2^2}{2\lambda f_0^2} \right) \exp\left( -\mathrm{j}2\pi \frac{x\omega_1 + y\omega_2}{\lambda f_0} \right) \mathrm{d}\omega_1 \mathrm{d}\omega_2$$

Optical parameters

- $\lambda$: wavelength (emission)
- $M$: magnification factor
- $f_0$: focal length
- $P(\omega_1,\omega_2) = \mathbb{1}_{\|\boldsymbol{\omega}\|<R_0}$: pupil function
- $\mathrm{NA} = n \sin\theta = R_0/f_0$: numerical aperture

# 2-D convolution model

Thin specimen $s(x,y)$ →  → $g(x,y) = (h_{2\mathrm{D}} * s)(x,y)$

- Airy disk: $h_{2\mathrm{D}}(x,y) = I_0 \left| 2\frac{J_1(r/r_0)}{r/r_0} \right|^2$

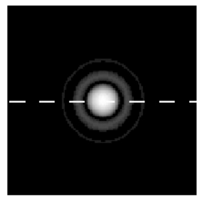

Radial profile

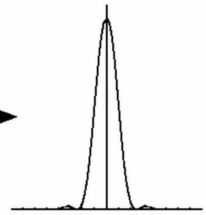

with $r = \sqrt{x^2+y^2}$, $r_0 = \frac{\lambda f_0}{2\pi R_0}$, $J_1(r)$: first-order Bessel function.

- Modulation transfer function

$$\hat{h}_{2\mathrm{D}}(\boldsymbol{\omega}) = \begin{cases} \frac{2}{\pi}\left(\arccos\left(\frac{\|\boldsymbol{\omega}\|}{\omega_0}\right) - \frac{\|\boldsymbol{\omega}\|}{\omega_0}\sqrt{1-\left(\frac{\|\boldsymbol{\omega}\|}{\omega_0}\right)^2}\right), & \text{for } 0 \le \|\boldsymbol{\omega}\| < \omega_0 \\ 0, & \text{otherwise} \end{cases}$$

Cut-off frequency (Rayleigh): $\omega_0 = \frac{2R_0}{\lambda f_0} = \frac{\pi}{r_0} \approx \frac{2\mathrm{NA}}{\lambda}$



# 2-D deconvolution: numerical set-up

- Discretization

$\omega_0 \le \pi$ and representation in (separable) sinc basis $\{\mathrm{sinc}(\boldsymbol{x}-\boldsymbol{k})\}_{\boldsymbol{k}\in\mathbb{Z}^2}$

Analysis functions: $\eta_{\boldsymbol{m}}(x,y) = h_{2\mathrm{D}}(x-m_1, y-m_2)$

$$\begin{aligned}[\mathbf{H}]_{\boldsymbol{m},\boldsymbol{k}} &= \langle \eta_{\boldsymbol{m}}, \mathrm{sinc}(\cdot - \boldsymbol{k})\rangle \\ &= \langle h_{2\mathrm{D}}(\cdot - \boldsymbol{m}), \mathrm{sinc}(\cdot - \boldsymbol{k})\rangle \\ &= \big(\mathrm{sinc} * h_{2\mathrm{D}}\big)(\boldsymbol{m}-\boldsymbol{k}) = h_{2\mathrm{D}}(\boldsymbol{m}-\boldsymbol{k}).\end{aligned}$$

$\mathbf{H}$ and $\mathbf{L}$: convolution matrices diagonalized by discrete Fourier transform

- Linear step of ADMM algorithm implemented using the FFT

$$\mathbf{s}^{k+1} = \left(\mathbf{H}^T\mathbf{H} + \mu\mathbf{L}^T\mathbf{L}\right)^{-1}\left(\mathbf{H}^T\mathbf{y} + \mathbf{z}^{k+1}\right)$$

with $\mathbf{z}^{k+1} = \mathbf{L}^T\left(\mu\mathbf{u}^k - \boldsymbol{\alpha}^k\right)$

# Deconvolution experiments

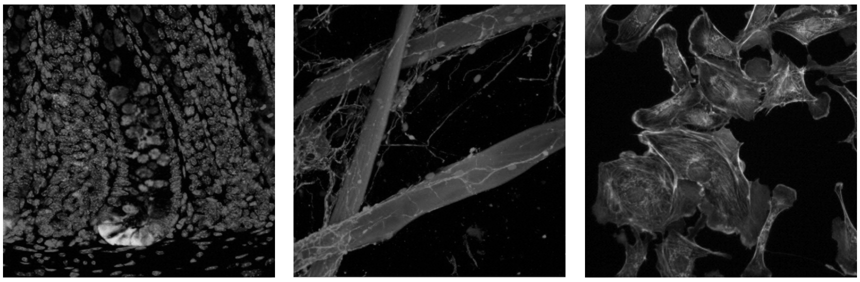

(a) (b) (c)

**Figure 10.3** Images used in deconvolution experiments. (a) Stem cells surrounded by goblet cells. (b) Nerve cells growing around fibers. (c) Artery cells.

**Table 10.2** Deconvolution performance of MAP estimators based on different prior distributions.

| | | Estimation performance (SNR in dB) | | |
|---|---|---|---|---|
| | BSNR (dB) | Gaussian | Laplace | Student's |
| Stem cells | 20 | **14.43** | 13.76 | 11.86 |
| | 30 | **15.92** | 15.77 | 13.15 |
| | 40 | **18.11** | **18.11** | 13.83 |
| Nerve cells | 20 | 13.86 | **15.31** | 14.01 |
| | 30 | 15.89 | **18.18** | 15.81 |
| | 40 | 18.58 | **20.57** | 16.92 |
| Artery cells | 20 | 14.86 | **15.23** | 13.48 |
| | 30 | 16.59 | **17.21** | 14.92 |
| | 40 | 18.68 | **19.61** | 15.94 |



# 2D deconvolution experiment

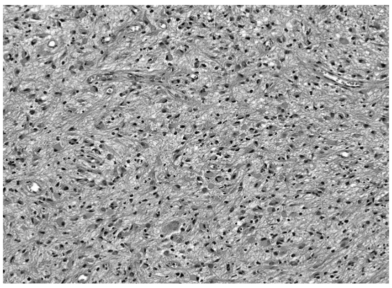

Astrocytes cells

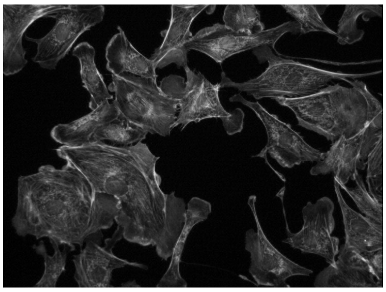

bovine pulmonary artery cells

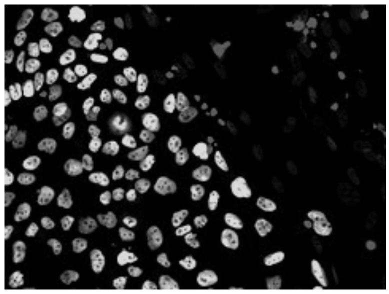

human embryonic stem cells

Disk shaped PSF (7x7)

$\mathrm{L}$ : gradient

Optimized parameters

Deconvolution results in dB

| | Gaussian Estimator | Laplace Estimator | Student's Estimator |
|---|---|---|---|
| Astrocytes cells | **12.18** | 10.48 | 10.52 |
| Pulmonary cells | 16.90 | **19.04** | 18.34 |
| Stem cells | 15.81 | 20.19 | **20.50** |

# Magnetic resonance imaging (MRI)

- Physical image formation model (noise-free)

$$\hat{s}(\boldsymbol{\omega}_m) = \int_{\mathbb{R}^2} s(\boldsymbol{r})\mathrm{e}^{-\mathrm{j}\langle \boldsymbol{\omega}_m, \boldsymbol{r}\rangle}\mathrm{d}\boldsymbol{r}$$

(sampling of Fourier transform)

Equivalent analysis function: $\eta_m(\boldsymbol{r}) = \mathrm{e}^{-\mathrm{j}\langle \boldsymbol{\omega}_m, \boldsymbol{r}\rangle}$

- Discretization in separable $\mathrm{sinc}$ basis

$$\begin{aligned}[\mathbf{H}]_{m,\boldsymbol{n}} &= \langle \eta_m, \mathrm{sinc}(\cdot - \boldsymbol{n})\rangle \\ &= \langle \mathrm{e}^{-\mathrm{j}\langle \boldsymbol{\omega}_m, \cdot\rangle}, \mathrm{sinc}(\cdot - \boldsymbol{n})\rangle = \mathrm{e}^{-\mathrm{j}\langle \boldsymbol{\omega}_m, \boldsymbol{n}\rangle}\end{aligned}$$

Property: $\mathbf{H}^T\mathbf{H}$ is circulant (FFT-based implementation)



# MRI: Shepp-Logan phantom

Original SL Phantom

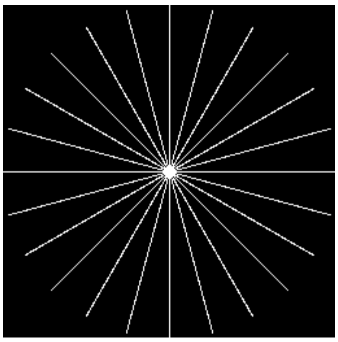

Fourier Sampling Pattern
12 Angles

Laplace prior (TV)

Student prior (log)

$\mathrm{L}$ : gradient
Optimized parameters

# MRI phantom: Spiral sampling in k-space

$\mathrm{L}$ : gradient

Optimized parameters

Original Phantom
(Guerquin-Kern TMI 2012)

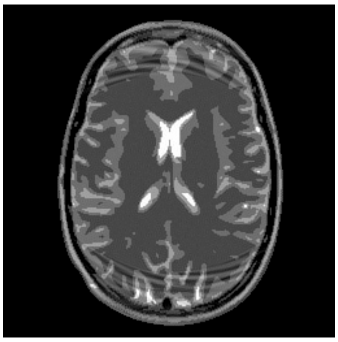

Gaussian prior (Tikhonov)
SER =17.69 dB

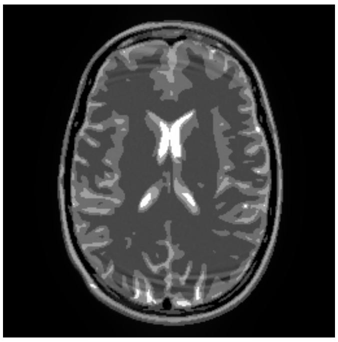

Laplace prior (TV)
SER = 21.37 dB

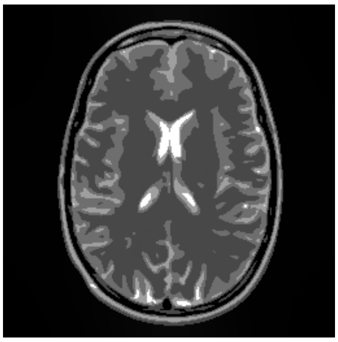

Student prior
SER = 27.22 dB



# MRI reconstruction experiments

(a) (b) (c)

**Figure 10.4** Data used in MR reconstruction experiments. (a) Cross section of a wrist. (b) Angiography image. (c) k-space sampling pattern along 40 radial lines.

**Table 10.3** MR reconstruction performance of MAP estimators based on different prior distributions.

| | Radial lines | Estimation performance (SNR in dB) | | |
|---|---|---|---|---|
| | | Gaussian | Laplace | Student's |
| Wrist | 20 | 8.82 | **11.8** | 5.97 |
| | 40 | 11.30 | **14.69** | 13.81 |
| Angiogram | 20 | 4.30 | 9.01 | **9.40** |
| | 40 | 6.31 | 14.48 | **14.97** |

# X-ray tomography

Projection geometry: $\boldsymbol{x} = t\boldsymbol{\theta} + r\boldsymbol{\theta}^{\perp}$ with $\boldsymbol{\theta} = (\cos\theta, \sin\theta)$

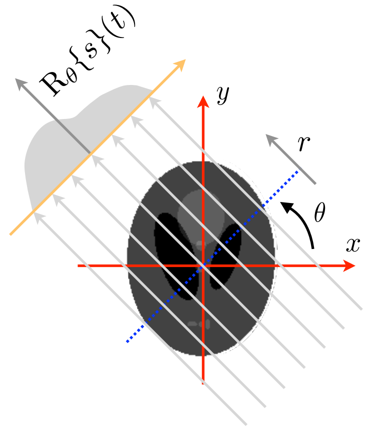


- Radon transform (line integrals)

$$\mathrm{R}_{\theta}\{s(\boldsymbol{x})\}(t) = \int_{\mathbb{R}} s(t\boldsymbol{\theta} + r\boldsymbol{\theta}^{\perp})\mathrm{d}r$$

$$= \int_{\mathbb{R}^2} s(\boldsymbol{x})\delta(t - \langle \boldsymbol{x}, \boldsymbol{\theta}\rangle)\mathrm{d}\boldsymbol{x}$$

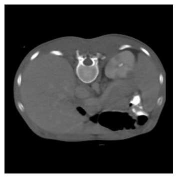

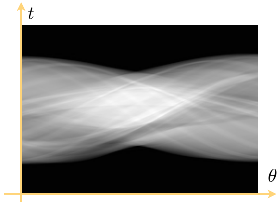


sinogram

Equivalent analysis functions: $\eta_m(\boldsymbol{x}) = \delta\big(t_m - \langle \boldsymbol{x}, \boldsymbol{\theta}_m\rangle\big)$



# Properties of Radon transform

- Projected translation invariance

$$\mathrm{R}_{\theta}\{\varphi(\cdot - \boldsymbol{x}_0)\}(t) = \mathrm{R}_{\theta}\{\varphi\}(t - \langle \boldsymbol{x}_0, \boldsymbol{\theta}\rangle)$$

- Pseudo-distributivity with respect to convolution

$$\mathrm{R}_{\theta}\{\varphi_1 * \varphi_2\}(t) = \left(\mathrm{R}_{\theta}\{\varphi_1\} * \mathrm{R}_{\theta}\{\varphi_2\}\right)(t)$$

- Fourier central-slice theorem

$$\int_{\mathbb{R}} \mathrm{R}_{\theta}\{\varphi\}(t)\mathrm{e}^{-\mathrm{j}\omega t}\mathrm{d}t = \hat{\varphi}(\boldsymbol{\omega})\big|_{\boldsymbol{\omega}=\omega\boldsymbol{\theta}}$$

$$\hat{p}_{\theta}(\omega) = \widehat{\mathrm{R}_{\theta}\{\varphi\}}(\omega) = \hat{\varphi}(\omega\cos\theta, \omega\sin\theta)$$

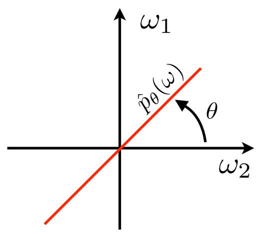


**Proposition**: Consider the separable function $\varphi(\boldsymbol{x}) = \varphi_1(x)\varphi_2(y)$. Then,

$$\mathrm{R}_{\theta}\{\varphi(\cdot - \boldsymbol{x}_0)\}(t) = \varphi_{\theta}(t - t_0)$$

where $t_0 = \langle \boldsymbol{x}_0, \boldsymbol{\theta}\rangle$ and

$$\varphi_{\theta}(t) = \left(\tfrac{1}{|\cos\theta|}\varphi_1\big(\frac{\cdot}{\cos\theta}\big) * \tfrac{1}{|\sin\theta|}\varphi_2\big(\frac{\cdot}{\sin\theta}\big)\right)(t).$$

# Spline flowers

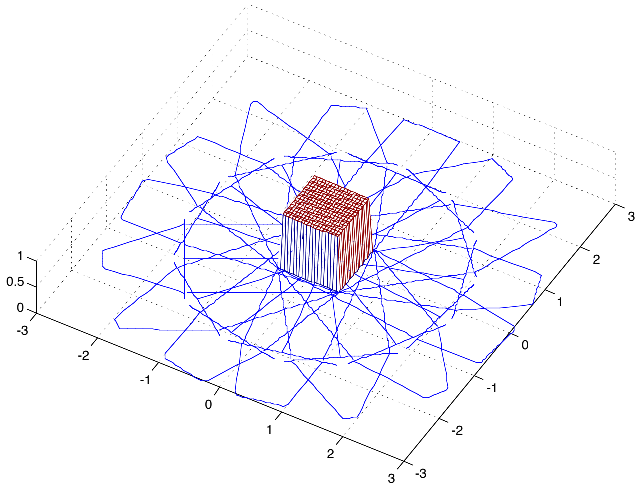

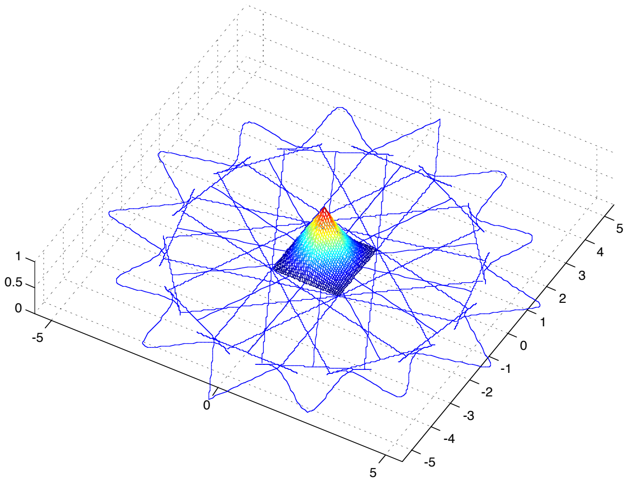



# X-ray tomography reconstruction results

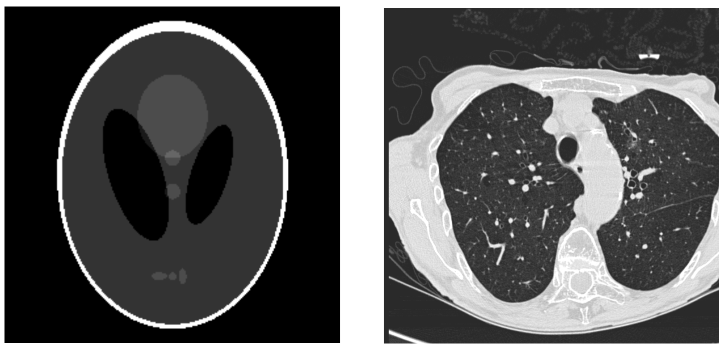

(a) (b)

**Figure 10.6** Images used in X-ray tomographic reconstruction experiments. (a) The Shepp-Logan (SL) phantom. (b) Cross section of a human lung.

**Table 10.4** Reconstruction results of X-ray computed tomography using different estimators.

| | Directions | Estimation performance (SNR in dB) | | |
|---|---|---|---|---|
| | | Gaussian | Laplace | Student's |
| SL Phantom | 120 | 16.8 | 17.53 | **18.76** |
| SL Phantom | 180 | 18.13 | 18.75 | **20.34** |
| Lung | 180 | **22.49** | 21.52 | 21.45 |
| Lung | 360 | **24.38** | 22.47 | 22.37 |